

## Macrocyclic Polyphosphane Ligands. Iron(II), Cobalt(II), and Nickel(II) Complexes of (4*RS*,7*RS*,13*SR*,16*SR*)-Tetraphenyl-1,10-dipropyl-1,10-diaza-4,7,13,16-tetraphosphacyclo-octadecane: Crystal Structures of their Tetraphenylborate Derivatives†

Carlo Mealli,\* Michal Sabat, and Fabrizio Zanobini

*Istituto per lo Studio della Stereochimica ed Energetica dei Composti di Coordinazione, C.N.R., Via F. D. Guerrazzi 27, 50132 Firenze, Italy*

Mario Ciampolini\* and Nicoletta Nardi

*Dipartimento di Chimica, Università di Firenze, Via J. Nardi 39, 50132 Firenze, Italy*

The chiral configuration of the title ligand,  $\beta$ -L<sup>1</sup>, and its co-ordinative behaviour towards iron(II), cobalt(II), and nickel(II) have been ascertained by determining the X-ray crystal structures of the low-spin complexes [Fe( $\beta$ -L<sup>1</sup>)] [BPh<sub>4</sub>]<sub>2</sub>·Me<sub>2</sub>NCHO (1), [Co( $\beta$ -L<sup>1</sup>)] [BPh<sub>4</sub>]<sub>2</sub>·Me<sub>2</sub>NCHO (2), and [Ni( $\beta$ -L<sup>1</sup>)] [BPh<sub>4</sub>]<sub>2</sub> (3). Complex (1) crystallises in the triclinic space group *P* $\bar{1}$ , with *a* = 15.156(3), *b* = 12.649(2), *c* = 13.333(3) Å,  $\alpha$  = 63.37(1),  $\beta$  = 61.44(2),  $\gamma$  = 68.01(1)°, and *Z* = 1. The iron atom is pseudo-octahedrally co-ordinated by the two nitrogen and four phosphorus atoms of the macrocycle. Complex (2) crystallises in the monoclinic space group *C2/c*, with *a* = 23.616(5), *b* = 13.078(4), *c* = 27.358(7) Å,  $\beta$  = 110.64(3)°, and *Z* = 4. The cobalt atom is co-ordinated by the four phosphorus atoms at normal bond distances of 2.265 Å (av.), whereas the nitrogen atoms are further (2.63 Å) from the metal. Complex (3) crystallises in the triclinic space group *P*1, with *a* = 13.581(2), *b* = 13.110(3), *c* = 13.483(2),  $\alpha$  = 118.45(2),  $\beta$  = 116.09(2),  $\gamma$  = 80.22(2)°, and *Z* = 1. The nickel atom is square planar, being co-ordinated by the four phosphorus atoms, whilst the two nitrogen atoms are definitely unco-ordinated at 3.27 Å. The structural rearrangement in the series of *d*<sup>6</sup>, *d*<sup>7</sup>, and *d*<sup>8</sup> compounds is interpreted in terms of progressively larger metal-axial ligand electronic repulsions.

This paper is part of a continuing study on the ligating capabilities of tetraphosphane macrocycles containing two additional donor groups E.<sup>1-6</sup> Due to the chirality of the phosphane groups, five different diastereoisomers of each macrocycle may exist and it is in principle possible to separate each one of them in a pure state (Figure 1). The co-ordinating capabilities of some diastereoisomers, containing sulphur or oxygen as E substituents, towards cobalt(II) and nickel(II) ions have been previously discussed.<sup>1,2,5,6</sup> By introducing amine groups into the macrocycle, the  $\sigma$  donor capabilities of the E substituents are expected to be enhanced. As a consequence, the metal-ligand interactions are orbital controlled to a great extent and those arrangements of the ligand that allow the highest covalency to the M-E bonds are then sought. On the other hand the fulfillment of the electronic requirements at the metal atom is somewhat contrasted by the steric requirements of the macrocycle in a particular chiral configuration.<sup>1,2</sup>

We have recently synthesised macrocycles of the series L<sup>1</sup> (see Figure 1).<sup>3</sup> The  $\gamma$ -diastereoisomer has already been investigated with regard to its chiral configuration and co-ordination capabilities towards cobalt(II) and nickel(II) ions.<sup>3,4</sup> Herein we report the results of the characterisation carried out for the iron(II), cobalt(II), and nickel(II) complexes of the  $\beta$ -diastereoisomer. In particular we are interested in ascertaining how the specific chirality of the ligand complies with the electron counts at the metal centre. X-Ray crystal-structure determinations have been carried out for the tetraphenylborate derivatives of iron, cobalt, and nickel.

### Results and Discussion

The present isomer,  $\beta$ -L<sup>1</sup>, is described previously as having a m.p. of 136–138 °C and a <sup>31</sup>P-<sup>1</sup>H n.m.r. chemical shift of –22.73 p.p.m.<sup>3</sup> The n.m.r. value suggests that the chiral configuration of the macrocycle could be either  $\beta$  or  $\delta$  (Figure 1).<sup>3</sup> The present crystal-structure determinations of the complexes [M( $\beta$ -L<sup>1</sup>)] [BPh<sub>4</sub>]<sub>2</sub> (M = Fe, Co, or Ni) show the chiral configurations of 4*RS*,7*RS*,13*SR*,16*SR* at the phosphorus atoms and thus justify its designation as the  $\beta$ -isomer (Figure 1) for the present diastereoisomer.

This macrocycle readily forms 1:1 complexes with iron, cobalt, and nickel. All the compounds described herein are low-spin: the iron and nickel complexes have a singlet ground state whereas the cobalt complexes have doublet ground states.

In order to ascertain the structural details of this macrocycle in its metal complexes the crystal and molecular structures of [Fe( $\beta$ -L<sup>1</sup>)] [BPh<sub>4</sub>]<sub>2</sub>·Me<sub>2</sub>NCHO (1), [Co( $\beta$ -L<sup>1</sup>)] [BPh<sub>4</sub>]<sub>2</sub>·Me<sub>2</sub>NCHO (2), and [Ni( $\beta$ -L<sup>1</sup>)] [BPh<sub>4</sub>]<sub>2</sub> (3) have been determined by X-ray analyses. Discrete tetraphenylborate anions and [M( $\beta$ -L<sup>1</sup>)]<sup>2+</sup> cations are present in the lattice of each compound. Interposed dimethylformamide solvent molecules are also found in the iron and cobalt derivatives.

Figures 2–4 show views of the three cations of iron, cobalt, and nickel, respectively. Selected bond distances and angles are reported in Table 1. These structural parameters must be evaluated with caution since all of the structures are affected by some amount of disorder. On the other hand, the main aim of our study was to determine the gross features of the co-ordinating capabilities of the ligand  $\beta$ -L<sup>1</sup> as a function of the nature of metal and we consider the results obtained suitable for the following discussion.

Whereas the MP<sub>4</sub> square-planar fragment is almost a common feature in all of the complexes, we observe that the amine donor atoms move progressively closer to the metal as the formal number of *d* electrons at the metal decreases from

† Supplementary data available (No. SUP 56114, 8 pp.): thermal parameters. See Instructions for Authors, *J. Chem. Soc., Dalton Trans.*, 1985, Issue 1, pp. xvii–xix. Structure factors are available from the editorial office.

Non-S.I. unit employed: B.M. = 0.927 × 10<sup>-23</sup> A m<sup>2</sup>.

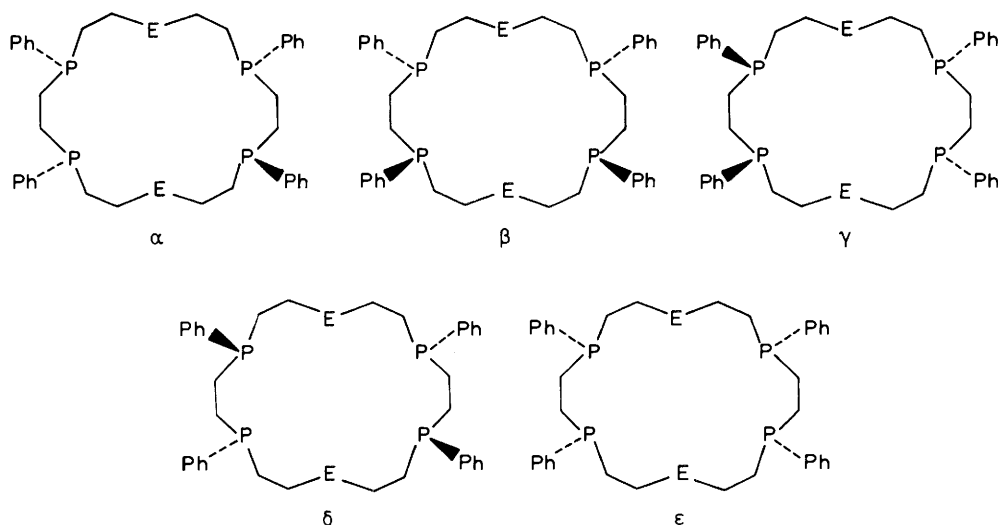


Figure 1. The five diastereoisomers of L [E = NPr ( $L^1$ ), O ( $L^2$ ), or S ( $L^3$ )]

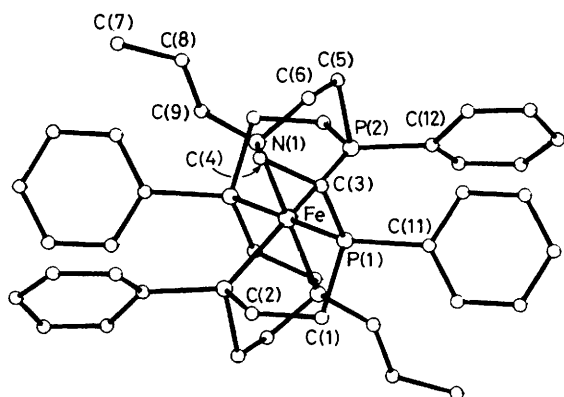


Figure 2. Perspective drawing of the complex cation  $[\text{Fe}(\beta\text{-L}^1)]^{2+}$  with the atom labelling scheme

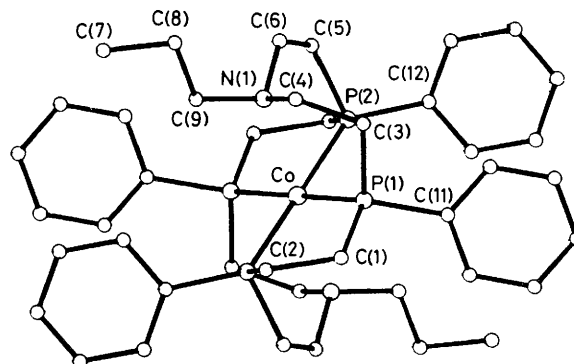


Figure 3. Perspective drawing of the complex cation  $[\text{Co}(\beta\text{-L}^1)]^{2+}$  with the atom labelling scheme

eight to six. In fact, the M–N distances drop from the non-bonding value of 3.30 (av.) in (3) to 2.63 in (2) and to 2.23 Å in (1), the last value undoubtedly indicating an operative bonding. The macrocyclic ligand allows such a geometrical rearrangement, which is clearly imposed by the electronic requirements of the metal centre.

In none of the compounds are the nitrogen atoms found at the zenith of the metal, but at best, an N–M–P angle of *ca.* 83° is achieved in the iron compound which is the most octahedral. The same angles have values of *ca.* 77 and 68° in (2) and (3), respectively, a fact which implies an increasing electronic rejection of nitrogen atoms from the co-ordination sphere. Also, as the M–N distances increase in going from (1) to (3) the P–M–P angles involving phosphorus atoms joined by the chain containing the amine group decrease. At the same time their adjacent P–M–P angles decrease. A difference of 20° between these two types of angles is found in (1) but this is reduced to only 6° in (3). This may be attributed to steric effects in the ligand.

In compound (3) there is an evident asymmetry of the Ni–P distances which range between 2.145(6) and 2.277(5) Å. On the other hand the molecule does not have any inner symmetry, not even a centre of symmetry, which in principle could be allowed by the particular  $\beta$ -configuration of the ligand. Reference to the molecules in Figure 4(a) and (b) clearly shows the lack of a

centre of symmetry. This is most clear when the propyl chains departing from the unco-ordinated nitrogen atoms are carefully observed.

Another interesting rearrangement, which is clearly induced in the ligand molecule by the particular co-ordination of the metal, regards the tilting of the P–C(Ph) bonds with respect to the  $\text{MP}_4$  co-ordination plane. In the nickel complex this angle is the largest (*ca.* 60°) but is progressively reduced as the nitrogens approach the metal in (2) and (1), respectively. In other words, the P–C(Ph) bonds are directed out of the co-ordination plane to comply with the new position of the nitrogen atoms that are entering the co-ordination sphere. The Fe–P distances in (1) are 2.309(2) and 2.288(3) Å. These values are consistent with a low-spin ground state of the molecule. In fact, it has been previously found in other complexes of iron(II) with a donor set of  $\text{P}_4\text{Cl}_2$ , that a dramatic lengthening of the Fe–P distances up to 2.68 Å occurs simultaneously with the occurrence of a quintet ground state.<sup>7,8</sup>

Moreover, this diamagnetic iron(II) complex (1) exhibits a reflectance spectrum with two ligand-field bands at 15 900 and 23 500  $\text{cm}^{-1}$  and which is similar in shape to the spectra of diamagnetic *trans*-octahedral iron(II) complexes of the type  $\text{FeCl}_2\text{P}_4$  and  $\text{FeN}_2\text{P}_4$ . These two bands are assigned as  $^1A_{1g} \rightarrow ^1E_g$  and  $^1A_{1g} \rightarrow ^1A_{2g}$  transitions, respectively, in the limit of  $D_{4h}$  symmetry.<sup>8–10</sup>

The complex  $[\text{Co}(\beta\text{-L}^1)][\text{BPh}_4]_2 \cdot \text{Me}_2\text{NCHO}$  (2) shows a

**Table 1.** Selected bond distances (Å) and angles (°) with estimated standard deviations in parentheses for (1), (2), and (3)

	(1) <sup>a</sup>	(2)	(3) <sup>b</sup>
M-P(1)	2.309(2)	2.284(7)	2.145(6) [2.277(5)]
M-P(2)	2.288(3)	2.245(7)	2.230(6) [2.192(6)]
M-N	2.230(8)	2.629(12)	3.269(5) [3.327(5)]
P(1)-C(1)	1.837(11)	1.831(27)	1.903(21) [1.792(17)]
P(1)-C(3)	1.847(12)	1.876(27)	1.918(17) [1.755(15)]
P(1)-C(11)	1.813(10)	1.821(18)	1.850(12) [1.791(12)]
P(2)-C(2A)	1.916(13) [1.801(14)]	1.829(29)	1.876(16) [1.870(18)]
P(2)-C(5)	1.848(12)	1.813(30)	1.850(19) [1.875(27)]
P(2)-C(12)	1.881(23) [1.780(27)]	1.787(23)	1.869(10) [1.777(11)]
	(1) <sup>a</sup>	(2)	(3) <sup>b</sup>
P(1)-M-P(2)	98.1(1)	96.0(3)	94.1(2) [92.1(2)]
P(1)-M-P(2A)	81.9(1)	84.0(1)	87.5(2) [86.3(2)]
N-M-P(1)	83.9(2)	77.3(7)	67.0(6) [64.9(6)]
N-M-P(2)	82.9(2)	79.1(7)	69.5(6) [71.5(6)]
M-P(1)-C(1)	112.1(3)	113.1(9)	107.7(7) [107.2(6)]
M-P(1)-C(3)	103.2(4)	108.7(9)	117.3(6) [132.2(6)]
M-P(1)-C(11)	133.1(3)	128.6(7)	114.1(4) [113.9(5)]
C(1)-P(1)-C(3)	101.5(5)	105.9(1.2)	110.5(8) [98.7(8)]
C(1)-P(1)-C(11)	100.8(4)	98.6(1.1)	105.0(7) [108.2(7)]
C(3)-P(1)-C(11)	101.8(5)	99.3(9)	101.5(5) [104.0(6)]
M-P(2)-C(2A)	107.8(3) [116.0(5)]	110.2(9)	110.2(5) [109.5(6)]
M-P(2)-C(5)	104.9(3)	109.1(1.0)	119.3(6) [122.2(8)]
M-P(2)-C(12)	124.4(8) [137.0(9)]	129.1(7)	111.1(4) [115.4(4)]
C(2A)-P(2)-C(5)	107.9(12) [93.3(14)]	98.9(11)	108.6(8) [99.2(11)]
C(2A)-P(2)-C(12)	102.5(10) [98.9(11)]	102.0(9)	100.0(6) [107.7(7)]
C(5)-P(2)-C(12)	108.5(8) [96.8(1)]	103.4(1.2)	105.9(6) [101.0(8)]

<sup>a</sup> Values in square brackets refer to bond lengths and angles for the disordered atoms marked by an asterisk in Table 2. <sup>b</sup> Values in square brackets refer to part A of the molecule: in (3) (non-centrosymmetric), part A is symmetry independent; in (1) and (2) it is related by an inversion centre to the other part of the molecule.

reflectance spectrum with bands at 9 600 and 19 000  $\text{cm}^{-1}$  which is similar to the spectra of *trans*-octahedral low-spin complexes such as  $[\text{Co}(\beta\text{-L}^2)][\text{BPh}_4]_2 \cdot 2\text{Me}_2\text{NCHO}$ , which has bands at 11 500 and 21 300  $\text{cm}^{-1}$ .<sup>1</sup> The remarkable red shift found for the present complex reflects the weaker ligand field due to the long Co-N bond distances in the strongly elongated octahedral chromophore. The magnetic moment of 2.26 B.M. in  $[\text{Co}(\beta\text{-L}^1)][\text{BPh}_4]_2 \cdot \text{Me}_2\text{NCHO}$  is rather high for an octahedral low-spin cobalt(II) complex (range 1.8–1.9 B.M.) and points towards the value for the planar cobalt(II) complexes (2.2–2.7 B.M.).<sup>11</sup>

A large blue shift is found in the reflectance spectrum of  $[\text{Co}(\beta\text{-L}^1)]\text{Br}_2$  ( $\mu_{\text{eff.}} = 2.03$  B.M.) which shows bands at 14 000 and 24 100  $\text{cm}^{-1}$ . Co-ordination of two bromide anions could account for such a spectrum, which is typical of low-spin octahedral cobalt(II) complexes. In dimethylformamide solution both the dibromide and bis(tetraphenylborate) complexes exhibit very similar absorption spectra with a peak at 15 000  $\text{cm}^{-1}$  ( $\epsilon$  32  $\text{dm}^3 \text{mol}^{-1} \text{cm}^{-1}$ ) and a shoulder at 24 500  $\text{cm}^{-1}$ , indicative of octahedral low-spin co-ordination. The co-ordination of the solvent molecules seems a reasonable hypothesis since conductivity measurements indicate that the complexes are present as 2:1 electrolytes in dimethylformamide.

Finally,  $[\text{Ni}(\beta\text{-L}^1)][\text{BPh}_4]_2$  (3) exhibits a reflectance spectrum with only a broad ligand-field band at 24 000  $\text{cm}^{-1}$ , in agreement with its square-planar structure.<sup>12</sup> The same ligand-field spectrum is shown by the dibromide analogue in the solid state. No significant spectral change is shown by both complexes when dissolved in dimethylformamide where they behave as 2:1 electrolytes. Thus they can be assigned to a square-planar  $\text{NiP}_4$  chromophore in solution as well. Conversely, there is some indication that the square-planar  $[\text{Ni}(\gamma\text{-L}^1)]^{2+}$  ion, in solution, may also take up a solvent

molecule or a bromide ion.<sup>4</sup> This different behaviour can be ascribed to the fact that the particular configuration of the  $\gamma$ -isomer forces the amine groups to stay away from the metal<sup>3</sup> whereas the same groups in the  $\beta$ -isomer, although unco-ordinated, may operate as effective shielding against the approach of any other intervening ligand.

## Conclusions

The present diastereoisomer,  $\beta\text{-L}^1$ , is able to act as a sixidentate ligand, imposing a *trans*-octahedral co-ordination in the iron complex (1). Thus electronic requirements, rather than configurational ones, are likely to be at the origin of the observed reduced co-ordinating capabilities of nitrogen in the cobalt and nickel complexes.

The co-ordination trends of the ligand  $\beta\text{-L}^1$  towards iron, cobalt, and nickel can be rationalised as follows by bearing in mind that all of the species are low-spin. The  $d^8$   $\text{Ni}^{\text{II}}$  complex (3) is highly stabilised by the square-planar environment. By assuming only  $\sigma$  donor capabilities for the phosphorus and nitrogen atoms of the macrocycle, it is clear that a 16-electron square-planar species is to be preferred over a 20-electron octahedral species. Clearly there would be four-electron repulsions between the nitrogen lone pairs and the filled metal  $d_{z^2}$  orbital, if the nitrogen atoms were located along the axis of an octahedron. The presence of the empty metal  $p_z$  orbital, that would allow some ligand-to-metal charge transfer, is not sufficient in this case to overcome the above destabilising interactions. In the case of the  $\text{Fe}^{\text{II}}$  complex (1),  $d_{z^2}$  is empty as well as is the  $p_z$  orbital: now the nitrogen lone pairs are in the presence of two potential accepting orbitals and may give rise to a stable 18-electron species if the macrocycle allows the necessary distortion to place the nitrogen donors at two vertices

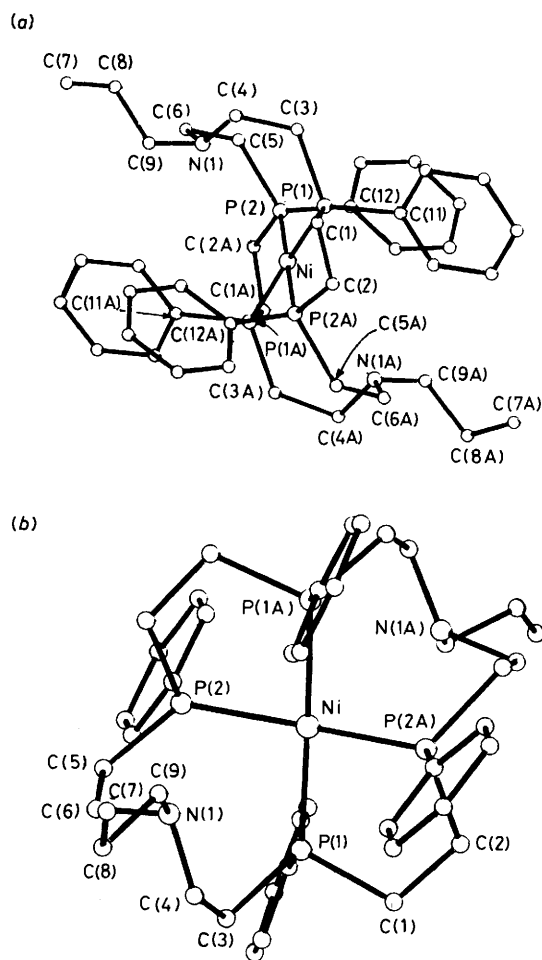


Figure 4. (a) Perspective drawing of the complex cation  $[\text{Ni}(\beta\text{-L}^1)]^{2+}$  with the atom labelling scheme; (b) view of the chelate ring conformation in  $[\text{Ni}(\beta\text{-L}^1)]^{2+}$

of the octahedron. The crystal-structure determination has shown that this is indeed possible. Finally, it was interesting to establish the co-ordination when the metal atom carries seven  $d$  electrons as in the case of the  $\text{Co}^{\text{II}}$  complex (2). It is in fact hard to predict whether the structure will remain square planar (as in the nickel analogue), or accept only one nitrogen donor to give rise to a square-pyramidal co-ordination, or, finally, form an improbable 19-electron octahedral species. The crystal-structure determination has shown that the co-ordination sphere is intermediate between those of the nickel and iron compounds. Although  $\text{Co-N}$  distances of 2.63(1) Å could in principle be considered as non-bonding, comparison with the nickel structure, where the nitrogen atoms are at 3.30(1) Å (mean) from

the metal, indirectly suggests a certain amount of metal-nitrogen interaction in (2).

Finally, it is noteworthy that the structures of the cobalt and nickel complexes of the ethereal,  $\text{L}^2$ ,<sup>7</sup> and thioetheral,  $\text{L}^3$ ,<sup>5</sup> analogues of the ligand  $\beta\text{-L}^1$  show  $\text{Co-O}$  and  $\text{Ni-S}$  distances of 2.35(1) and 2.94(1) Å, respectively. These values suggest stronger metal-ligand interactions when compared with 2.63(1) and 3.27(1) Å found for  $\text{Co-N}$  and  $\text{Ni-N}$  in the present series of structures. The arguments outlined above suggest repulsive orbital interactions between the nitrogen lone pairs and filled, or partially filled, metal orbitals. Thus we conclude that the lone pair in the ethereal and thioetheral groups is either more contracted and less directional than that of the amine, or the metal-ligand interaction is charge controlled to some extent.

### Experimental

**Syntheses of the Metal Complexes.**—The ligand was prepared as previously described.<sup>3</sup> The iron and cobalt complexes were prepared under a nitrogen atmosphere. The yields of recrystallised complexes were in the range 70–80%. Analytical and physical data are given in Table 2.

$[\text{M}(\beta\text{-L}^1)][\text{BPh}_4]_2 \cdot x\text{Me}_2\text{NCHO}$ . A solution of  $\text{M}(\text{BPh}_4)_2 \cdot 6\text{H}_2\text{O}$  (0.1 mmol) in ethanol-water (5 cm<sup>3</sup>, 1:1 v/v) was added to a solution of the ligand (0.1 mmol) in acetone (25 cm<sup>3</sup>). Crystals separated which were filtered off, washed with acetone, and dried *in vacuo*. The compounds were recrystallised from dimethylformamide-ethanol (1:1 v/v).

$[\text{M}(\beta\text{-L}^1)]\text{Br}_2$ . A solution of  $\text{MBr}_2$  (0.1 mmol) in ethanol-water (5 cm<sup>3</sup>, 2:1 v/v) was added to a solution of the ligand (1.1 mmol) in acetone (20 cm<sup>3</sup>). The resulting solution was evaporated to ca. 10 cm<sup>3</sup> and left overnight. Crystals separated which were filtered off, washed with acetone, and dried *in vacuo*.

**Physical Measurements.**—Visible and u.v. spectra were recorded on solutions with a Cary 17 and on solids with a Beckman DK-2 spectrophotometer. Magnetic susceptibility measurements were carried out with a Faraday balance. Electrical conductivity values were measured on a WTW conductance bridge at 25 °C. Concentrations of the solutions were ca. 10<sup>-3</sup> mol dm<sup>-3</sup>.

**X-Ray Crystallographic Studies.**—All X-ray measurements were performed on a Philips PW 1100 diffractometer using  $\text{Mo-K}_\alpha$  radiation ( $\lambda = 0.71069$  Å).

**Crystal data.** (1)  $\text{C}_{93}\text{H}_{105}\text{B}_2\text{FeN}_3\text{OP}_4$ ,  $M = 1482.25$ , triclinic,  $a = 15.156(3)$ ,  $b = 12.649(2)$ ,  $c = 13.333(3)$  Å,  $\alpha = 63.37(1)$ ,  $\beta = 61.44(2)$ ,  $\gamma = 68.01(1)^\circ$ ,  $U = 1965$  Å<sup>3</sup> (by least-squares refinement on setting angles for 25 reflections), space group  $P\bar{1}$  (no. 2),  $Z = 1$ ,  $D_c = 1.252$  g cm<sup>-3</sup>,  $F(000) = 788$ . Crystal habit and dimensions: olive-green needle,  $0.08 \times 0.1 \times 0.32$  mm,  $\mu(\text{Mo-K}_\alpha) = 3.19$  cm<sup>-1</sup>.

(2)  $\text{C}_{93}\text{H}_{105}\text{B}_2\text{CoN}_3\text{OP}_4$ ,  $M = 1485.34$ , monoclinic,  $a = 23.616(5)$ ,  $b = 13.078(4)$ ,  $c = 27.358(7)$  Å,  $\beta = 110.64(3)^\circ$ ,  $U =$

Table 2. Analytical and physical data for complexes of  $\text{L}^1$

Compound	Colour	Analysis <sup>a</sup> (%)			$\Lambda^b/\Omega^{-1} \text{ cm}^2 \text{ mol}^{-1}$
		C	H	N	
(1) $[\text{Fe}(\beta\text{-L}^1)][\text{BPh}_4]_2 \cdot \text{Me}_2\text{NCHO}$	Olive-green	75.5 (73.35)	7.3 (7.15)	2.9 (2.85)	104
(2) $[\text{Co}(\beta\text{-L}^1)][\text{BPh}_4]_2 \cdot \text{Me}_2\text{NCHO}$	Brown	75.3 (75.2)	7.4 (7.15)	2.8 (2.85)	98
$[\text{Co}(\beta\text{-L}^1)]\text{Br}_2$	Green	53.7 (54.05)	6.4 (6.25)	3.1 (3.00)	115
(3) $[\text{Ni}(\beta\text{-L}^1)][\text{BPh}_4]_2$	Yellow	76.6 (76.55)	7.2 (7.00)	2.0 (2.00)	101
$[\text{Ni}(\beta\text{-L}^1)]\text{Br}_2$	Orange	54.4 (54.05)	6.5 (6.25)	3.1 (3.00)	94

<sup>a</sup> Calculated values are given in parentheses. <sup>b</sup> Molar conductance values for ca. 10<sup>-3</sup> mol dm<sup>-3</sup> dimethylformamide solutions at 20 °C.

**Table 3.** Fractional atomic co-ordinates ( $\times 10^4$ ) with estimated standard deviations in parentheses for (1)

Atom	x	y	z	Atom	x	y	z
Fe	0	0	0	C(22)*	-2 862(20)	-730(24)	202(26)
P(1)	-1 052(2)	1 654(2)	596(3)	C(32)*	-3 964(19)	-429(24)	581(26)
P(2)	-972(2)	-146(2)	-801(3)	C(42)*	-4 460(20)	717(25)	229(27)
N(1)	551(6)	1 388(7)	-1 809(7)	C(52)*	-3 935(25)	1 624(24)	-574(32)
C(1)	-584(7)	2 000(10)	1 436(9)	C(62)*	-2 807(22)	1 318(25)	-934(27)
C(2)	604(8)	1 772(21)	797(21)	B(1)	1 780(9)	3 043(11)	2 468(11)
C(3)	-798(9)	2 933(11)	-839(10)	C(13)	534(5)	2 930(4)	3 208(5)
C(4)	-303(15)	2 475(16)	-1 904(16)	C(23)	-224(5)	3 973(4)	3 061(5)
C(5)	-549(8)	853(11)	-2 393(11)	C(33)	-1 256(5)	3 894(4)	3 632(5)
C(6)	495(7)	1 126(9)	-2 755(9)	C(43)	-1 530(5)	2 772(4)	4 349(5)
C(7)	2 944(19)	2 699(30)	-3 674(28)	C(53)	-773(5)	1 729(4)	4 496(5)
C(8)	1 848(18)	2 670(23)	-3 430(19)	C(63)	259(5)	1 808(4)	3 925(5)
C(9)	1 504(12)	1 736(21)	-2 145(18)	C(14)	2 526(6)	1 707(7)	2 920(7)
C(2)*	569(10)	1 479(22)	1 210(24)	C(24)	2 655(6)	764(7)	2 557(7)
C(4)*	218(12)	2 625(19)	-1 831(16)	C(34)	3 202(6)	-381(7)	3 013(7)
C(7)*	3 466(17)	1 668(27)	-3 649(25)	C(44)	3 620(6)	-582(7)	3 831(7)
C(8)*	2 331(16)	1 857(22)	-3 441(17)	C(54)	3 491(6)	360(7)	4 193(7)
C(9)*	1 704(8)	1 095(19)	-2 160(16)	C(64)	2 944(6)	1 505(7)	3 738(7)
C(11)	-2 427(8)	2 076(9)	1 352(9)	C(15)	2 135(4)	3 467(6)	950(6)
C(21)	-2 900(19)	1 818(22)	2 590(22)	C(25)	3 178(4)	3 251(6)	240(6)
C(31)	-3 961(20)	2 078(24)	3 179(23)	C(35)	3 500(4)	3 641(6)	-1 016(6)
C(41)	-4 585(10)	2 757(12)	2 448(13)	C(45)	2 779(4)	4 246(6)	-1 563(6)
C(51)	-4 099(24)	3 205(28)	1 241(28)	C(55)	1 736(4)	4 461(6)	-853(6)
C(61)	-3 035(23)	2 913(27)	662(27)	C(65)	1 414(4)	4 072(6)	404(6)
C(21)*	-2 949(17)	2 920(20)	973(21)	C(16)	1 992(5)	4 097(6)	2 740(5)
C(31)*	-4 010(19)	3 605(23)	1 498(23)	C(26)	2 876(5)	4 576(6)	1 987(5)
C(51)*	-4 098(19)	1 497(22)	2 839(22)	C(36)	3 086(5)	5 373(6)	2 266(5)
C(61)*	-3 031(19)	1 194(22)	2 288(22)	C(46)	2 411(5)	5 691(6)	3 299(5)
C(12)	-2 414(18)	142(21)	-148(23)	C(56)	1 527(5)	5 212(6)	4 053(5)
C(22)	-2 921(21)	-849(25)	606(26)	C(66)	1 318(5)	4 415(6)	3 773(5)
C(32)	-3 988(20)	-630(24)	1 101(26)	N(2)	5 000	5 000	5 000
C(42)	-4 544(17)	591(21)	850(23)	C(10)	5 536(31)	4 700(44)	5 660(35)
C(52)	-4 032(15)	1 565(18)	102(20)	C(11)	4 715(41)	6 301(12)	4 485(56)
C(62)	-2 970(15)	1 339(18)	-357(20)	C(12)	5 083(44)	4 169(50)	4 467(53)
C(12)*	-2 297(21)	187(25)	-547(26)	O(1)	5 630(37)	3 607(42)	6 215(45)

Atoms labelled with an asterisk refer to the alternative positions due to disorder.

**Table 4.** Fractional atomic co-ordinates ( $\times 10^4$ ) with estimated standard deviations in parentheses for (2)

Atom	x	y	z	Atom	x	y	z
Co	2 500	2 500	5 000	C(23)	688(7)	626(14)	691(5)
P(1)	2 412(4)	3 958(6)	4 519(3)	C(33)	550(7)	-330(14)	846(5)
P(2)	3 041(4)	1 624(6)	4 610(3)	C(43)	795(7)	-619(14)	1 370(5)
N(1)	3 570(9)	3 353(18)	5 429(8)	C(53)	1 177(7)	46(14)	1 738(5)
B(1)	1 226(12)	2 437(28)	881(9)	C(63)	1 315(7)	1 002(14)	1 582(5)
C(1)	1 997(11)	4 975(23)	4 708(10)	C(14)	730(7)	3 317(12)	978(6)
C(2)	2 041(12)	4 751(22)	5 312(11)	C(24)	545(7)	3 185(12)	1 406(6)
C(3)	3 188(12)	4 483(24)	4 637(10)	C(34)	176(7)	3 914(12)	1 516(6)
C(4)	3 572(13)	4 396(19)	5 220(10)	C(44)	-10(7)	4 775(12)	1 198(6)
C(5)	3 839(15)	1 752(25)	4 994(12)	C(54)	175(7)	4 907(12)	770(6)
C(6)	4 034(12)	2 730(22)	5 321(12)	C(64)	544(7)	4 178(12)	661(6)
C(7)	4 464(19)	4 027(36)	6 852(14)	C(15)	1 937(8)	2 756(13)	1 251(6)
C(8)	4 363(14)	3 963(29)	6 263(13)	C(25)	2 080(8)	3 746(13)	1 446(6)
C(9)	3 734(13)	3 469(25)	6 001(8)	C(35)	2 681(8)	4 011(13)	1 719(6)
C(11)	2 087(6)	4 117(14)	3 813(7)	C(45)	3 139(8)	3 287(13)	1 798(6)
C(21)	2 459(6)	4 228(14)	3 518(7)	C(55)	2 995(8)	2 297(13)	1 603(6)
C(31)	2 203(6)	4 341(14)	2 977(7)	C(65)	2 394(8)	2 032(13)	1 330(6)
C(41)	1 575(6)	4 341(14)	2 731(7)	C(16)	1 140(5)	2 461(13)	245(5)
C(51)	1 204(6)	4 230(14)	3 027(7)	C(26)	1 645(5)	2 358(13)	96(5)
C(61)	1 459(6)	4 117(14)	3 568(7)	C(36)	1 571(5)	2 301(13)	-433(5)
C(12)	3 019(7)	1 704(16)	3 952(8)	C(46)	993(5)	2 348(13)	-812(5)
C(22)	3 535(7)	1 548(16)	3 824(8)	C(56)	488(5)	2 451(13)	-663(5)
C(32)	3 489(7)	1 527(16)	3 302(8)	C(66)	562(5)	2 508(13)	-134(5)
C(42)	2 928(7)	1 662(16)	2 907(8)	C(10)	5 000	2 622(41)	2 500
C(52)	2 412(7)	1 818(16)	3 034(8)	N(2)	5 000	1 620(41)	2 500
C(62)	2 458(7)	1 839(16)	3 557(8)	C(11)	4 654(18)	1 959(37)	2 818(15)
C(13)	1 070(7)	1 292(14)	1 058(5)	O(1)	5 092(29)	3 342(38)	2 246(22)

**Table 5.** Fractional atomic co-ordinates ( $\times 10^4$ ) with estimated standard deviations in parentheses for (3)

Atom	x	y	z	Atom	x	y	z
Ni	0	0	0	C(62A)	-2 303(9)	-998(11)	-4 135(7)
P(1)	547(5)	1 740(5)	664(6)	C(15)	7 900(9)	1 786(9)	4 697(11)
P(1A)	-553(5)	-1 860(5)	-717(5)	C(25)	6 929(9)	1 551(9)	3 633(11)
P(2)	502(5)	185(6)	1 892(5)	C(35)	6 648(9)	421(9)	2 674(11)
P(2A)	-485(6)	-240(5)	-1 881(6)	C(45)	7 338(9)	-475(9)	2 780(11)
B(1)	8 229(22)	3 150(25)	5 933(25)	C(55)	8 309(9)	-240(9)	3 844(11)
B(2)	-8 172(15)	-3 203(16)	-5 916(16)	C(65)	8 590(9)	890(9)	4 803(11)
N(1)	-1 403(12)	1 970(13)	1 392(14)	C(16)	9 541(10)	3 425(13)	6 867(8)
N(1A)	1 501(11)	-2 037(12)	-1 267(12)	C(26)	10 293(10)	3 059(13)	6 332(8)
C(1)	-128(17)	2 115(18)	-685(18)	C(36)	11 414(10)	3 303(13)	7 082(8)
C(1A)	207(14)	-2 259(14)	509(15)	C(46)	11 783(10)	3 914(13)	8 368(8)
C(2)	-50(14)	1 087(15)	-1 799(16)	C(56)	11 031(10)	-4 280(13)	8 903(9)
C(2A)	286(12)	-1 241(13)	1 797(14)	C(66)	9 910(10)	4 036(13)	8 152(8)
C(3)	339(11)	2 930(16)	2 089(16)	C(17)	7 432(10)	3 346(8)	6 730(10)
C(3A)	-291(11)	-3 054(14)	-1 910(14)	C(27)	6 981(10)	2 440(8)	6 690(10)
C(4)	-927(11)	3 064(13)	1 655(15)	C(37)	6 383(10)	2 684(8)	7 387(10)
C(4A)	840(11)	-3 146(12)	-1 947(15)	C(47)	6 235(10)	3 833(8)	8 125(10)
C(5)	-86(13)	1 332(18)	2 929(16)	C(57)	6 686(10)	4 740(8)	8 165(10)
C(5A)	111(17)	-1 372(26)	-2 950(25)	C(67)	7 284(10)	4 496(8)	7 468(10)
C(6)	-1 287(15)	1 593(22)	2 316(19)	C(18)	7 793(7)	2 075(10)	5 278(10)
C(6A)	1 249(14)	-1 758(17)	-2 303(15)	C(28)	6 695(7)	4 352(10)	4 852(10)
C(7)	-4 348(17)	3 208(23)	553(23)	C(38)	6 361(7)	5 085(10)	4 290(10)
C(7A)	4 500(14)	-2 792(18)	-197(18)	C(48)	7 124(7)	5 541(10)	4 154(10)
C(8)	-3 187(19)	3 001(24)	1 345(22)	C(58)	8 221(7)	5 265(10)	4 581(10)
C(8A)	3 334(15)	-2 960(20)	-1 225(17)	C(68)	8 556(7)	4 532(10)	5 143(10)
C(9)	-2 592(14)	1 973(21)	689(20)	C(19)	-7 961(8)	-1 843(8)	-4 819(10)
C(9A)	2 674(11)	-2 096(16)	-518(15)	C(29)	-6 962(8)	-1 551(8)	-3 778(10)
C(11)	2 040(9)	1 925(9)	1 173(9)	C(39)	-6 693(8)	-398(8)	-2 872(10)
C(21)	2 730(9)	2 747(9)	2 340(9)	C(49)	-7 422(8)	463(8)	-3 007(10)
C(31)	3 842(9)	2 854(9)	2 635(9)	C(59)	-8 421(8)	171(8)	-4 049(10)
C(41)	4 642(9)	2 138(9)	1 763(9)	C(69)	-8 690(8)	-982(8)	-4 954(10)
C(51)	3 572(9)	1 316(9)	597(9)	C(110)	-9 530(9)	-3 509(11)	-6 871(8)
C(61)	2 461(9)	1 209(9)	302(9)	C(210)	-10 318(9)	-3 134(11)	-6 385(8)
C(11A)	-1 986(9)	-2 050(11)	-1 159(9)	C(310)	-11 429(9)	-3 415(11)	-7 176(8)
C(21A)	-2 663(9)	-2 721(11)	-2 403(9)	C(410)	-11 751(9)	-4 070(11)	-8 451(8)
C(31A)	-3 783(9)	-2 871(11)	-2 770(9)	C(510)	-10 963(9)	-4 445(11)	-8 937(8)
C(41A)	-4 227(9)	-2 350(11)	-1 893(9)	C(610)	-9 853(9)	-4 165(11)	-8 146(8)
C(51A)	-3 550(9)	-1 679(11)	-649(9)	C(111)	-7 483(10)	-3 389(8)	-6 722(11)
C(61A)	-2 429(9)	-1 529(11)	-281(9)	C(211)	-7 147(10)	-2 416(8)	-6 681(11)
C(12)	2 025(8)	405(11)	2 786(8)	C(311)	-6 550(10)	-2 550(8)	-7 349(11)
C(22)	2 650(8)	-17(11)	2 093(8)	C(411)	-6 288(10)	-3 656(8)	-8 059(11)
C(32)	3 790(8)	159(11)	2 691(8)	C(511)	-6 624(10)	-4 628(8)	-8 099(11)
C(42)	4 305(8)	755(11)	3 981(8)	C(611)	-7 221(10)	-4 495(8)	-7 431(11)
C(52)	3 679(8)	1 177(11)	4 674(8)	C(112)	-7 720(10)	-4 180(12)	-5 298(13)
C(62)	2 538(8)	1 001(11)	4 076(8)	C(212)	-6 603(10)	-4 388(12)	-4 874(13)
C(12A)	-1 912(9)	-524(11)	-2 851(7)	C(312)	-6 194(10)	-5 101(12)	-4 290(13)
C(22A)	-2 649(9)	-224(11)	-2 300(7)	C(412)	-6 902(10)	-5 607(12)	-4 129(13)
C(32A)	-3 776(9)	-398(11)	-3 035(7)	C(512)	-8 019(10)	-5 399(12)	-4 554(13)
C(42A)	-4 167(9)	-872(11)	-4 320(7)	C(612)	-8 427(10)	-4 686(12)	-5 138(13)
C(52A)	-3 430(9)	-1 172(11)	-4 870(7)				

7 907 Å<sup>3</sup> (from setting angles for 22 reflections), space group *C2/c* (no. 15),  $Z = 4$ ,  $D_c = 1.247 \text{ g cm}^{-3}$ ,  $F(000) = 3 152$ . Crystal habit and dimensions: red parallelepiped,  $0.08 \times 0.1 \times 0.12 \text{ mm}$ ,  $\mu(\text{Mo-K}\alpha) = 3.43 \text{ cm}^{-1}$ .

(3)  $\text{C}_{90}\text{H}_{98}\text{B}_2\text{N}_2\text{NiP}_4$ ,  $M = 1 412.01$ , triclinic,  $a = 13.581(2)$ ,  $b = 13.110(3)$ ,  $c = 13.483(2) \text{ \AA}$ ,  $\alpha = 118.45(2)$ ,  $\beta = 116.09(2)$ ,  $\gamma = 80.22(2)^\circ$ ,  $U = 1 893 \text{ \AA}^3$  (from setting angles for 21 reflections), space group *P1* (no. 1),  $Z = 1$ ,  $D_c = 1.238 \text{ g cm}^{-3}$ ,  $F(000) = 750$ . Crystal habit and dimensions: yellow-orange needle,  $0.12 \times 0.21 \times 0.435 \text{ mm}$ ,  $\mu(\text{Mo-K}\alpha) = 3.85 \text{ cm}^{-1}$ .

**Data collection.** (1)  $\omega/2\theta$  mode with scan width =  $0.70 + 0.30 \tan\theta$ , and scan speed  $0.07^\circ \text{ s}^{-1}$ . 5 376 Reflections measured ( $5 \leq 2\theta \leq 46^\circ$ ), 2 274 with  $I > 3\sigma(I)$  used in calculations. (2)  $\omega/2\theta$  mode, scan width  $0.8^\circ$ , scan speed  $0.05^\circ \text{ s}^{-1}$ . 3 982 Reflections measured ( $5 \leq 2\theta \leq 40^\circ$ ), 1 035 with  $I > 3\sigma(I)$  used in the calculations. (3)  $\omega/2\theta$  mode, scan width  $0.8^\circ$ , scan speed  $0.06^\circ \text{ s}^{-1}$ . 6 341 Reflections measured ( $5 \leq 2\theta \leq 50^\circ$ ), 3 485

with  $I > 3\sigma(I)$  used in the calculations. Three standard reflections were monitored every 120 min during each of the data collections. In no case was significant deviation of the control intensities observed. The intensities measured were corrected for Lorentz and polarisation effects. Absorption corrections have not been applied since the maximum and minimum transmission factors were not significantly different (5% at most) in any case.

**Solution and refinement of the structure.** The structures have been solved by means of the heavy-atom technique using the SHELX 76 program package.<sup>13</sup> From the Patterson maps it was clear that the metal atoms lie at centres of symmetry in both (1) and (2), (3) has a non-centrosymmetric structure; however the co-ordination polyhedron is almost centrosymmetric and in the beginning the nickel atom was fixed at the position 0,0,0. This constraint was also maintained at later stages of the structure solution and refinement, although the crystallographic centre of

inversion was dismissed. In fact a sufficiently good refinement was obtained only in the space group  $P1$ . From early stages, inspection of the Fourier maps showed that practically all of the structures suffer from disorder. In the case of the iron derivative (1) it was possible to recognise the alternative atom positions and both conformations were refined with occupancy factors of 0.5 for all of the disordered atoms. The disorder affects mainly the side chains of the ligand including the propyl groups and the phenyl rings. A similar phenomenon has been observed previously for the cobalt complex with an ethereal analogue ( $\beta$ -L<sup>2</sup>) of the present ligand.<sup>2</sup> In the case of the nickel and cobalt derivatives an overlap of the peaks corresponding to the alternative conformations precluded more detailed analysis. However, many atoms of the complex ions were characterised by high thermal parameters. Furthermore, earlier stages of the refinement resulted in rather poorly defined geometries of the species. Since the bond distances and angles in the three structures were found to be affected by the disorder phenomena certain constraints were adopted during the refinement. Thus not only the phenyl rings were imposed by the  $D_{6h}$  symmetry, with C–C distances of 1.395 Å, but also the C–C and C–N bonds in the ligand molecule which were fixed at values of 1.54 and 1.48 Å, respectively. The final results of a full-matrix least-squares refinement with the constraints described above were as follows: (1)  $R = 0.089$ ,  $R' = 0.092$ ; (2)  $R = 0.087$ ,  $R' = 0.090$ ; (3)  $R = 0.072$ ,  $R = 0.079$ , where  $R' = \sum w(|F_o| - |F_c|)^2 / \sum w|F_o|^2$ . The function refined was of the form  $\sum w(|F_o| - |F_c|)^2$  with weights  $w^{-1} = [\sigma^2(F) + pF^2]$  where the parameter  $p$  was chosen as 0.0008, 0.002, and 0.005, respectively, for (1), (2), and (3). The number of refined parameters was 244 for (1), 155 for (2), and 285 for (3). The contributions from the hydrogen atoms (in their idealised positions, C–H 1.08 Å) attached to the carbon atoms which were not affected by disorder have been included in the calculations. During the later stages of the refinements the metal and phosphorus atoms were assigned anisotropic thermal parameters. Atomic scattering factors were those tabulated by Cromer and Waber<sup>14</sup> with anomalous dispersion corrections taken from ref. 15. In the case of the iron and cobalt derivatives difference maps revealed some higher peaks which were ascribed to disordered molecules of dimethylformamide. During the refinement the interatomic distances within the dimethylformamide molecules were kept fixed at 1.45, 1.31,

and 1.23 Å for the N–C(CH<sub>3</sub>), N–C(O), and C–O bonds, respectively. The final atomic parameters are listed in Tables 3–5.

### Acknowledgements

Thanks are expressed to Mr. D. Masi for technical assistance in the X-ray work and to Mr. F. Cecconi for magnetic measurements.

### References

- 1 M. Ciampolini, P. Dapporto, N. Nardi, and F. Zanobini, *J. Chem. Soc., Chem. Commun.*, 1980, 177; M. Ciampolini, P. Dapporto, A. Dei, N. Nardi, and F. Zanobini, *Inorg. Chem.*, 1982, **21**, 489.
- 2 M. Ciampolini, P. Dapporto, N. Nardi, and F. Zanobini, *Inorg. Chem.*, 1983, **22**, 13.
- 3 M. Ciampolini, N. Nardi, F. Zanobini, R. Cini, and P. L. Orioli, *Inorg. Chim. Acta*, 1983, **76**, L17.
- 4 S. Mangani, P. L. Orioli, M. Ciampolini, N. Nardi, and F. Zanobini, *Inorg. Chim. Acta*, 1984, **85**, 65.
- 5 M. Ciampolini, N. Nardi, P. Dapporto, P. Innocenti, and F. Zanobini, *J. Chem. Soc., Dalton Trans.*, 1984, 575.
- 6 M. Ciampolini, N. Nardi, P. Dapporto, and F. Zanobini, *J. Chem. Soc., Dalton Trans.*, 1984, 995.
- 7 F. Cecconi, M. Di Vaira, S. Midollini, A. Orlandini, and L. Sacconi, *Inorg. Chem.*, 1981, **20**, 3423.
- 8 M. Di Vaira, S. Midollini, and L. Sacconi, *Inorg. Chem.*, 1981, **20**, 3430.
- 9 R. S. Feltham and W. Silverthorn, *Inorg. Chem.*, 1968, **7**, 1154; W. Levason, C. A. McAuliffe, M. Mahfooz Khan, and S. M. Nelson, *J. Chem. Soc., Dalton Trans.*, 1975, 1778.
- 10 A. B. P. Lever, *Coord. Chem. Rev.*, 1968, **3**, 119.
- 11 R. L. Carlin, *Transition Met. Chem.*, 1965, **1**, 1; F. A. Cotton and G. Wilkinson, 'Advanced Inorganic Chemistry,' Interscience, John Wiley and Sons, New York, 1980, p. 772.
- 12 C. Furlani, *Coord. Chem. Rev.*, 1968, **3**, 141.
- 13 G. M. Sheldrick, SHELX 76, Program for Crystal Structure Determinations, University of Cambridge, 1976.
- 14 'International Tables for X-Ray Crystallography,' Kynoch Press, Birmingham, 1974, vol. 4, p. 99.
- 15 Ref. 14, p. 149.

Received 12th April 1984; Paper 4/608